



Quantum many-body scars and weak breaking of ergodicity

Maksym Serbyn¹, Dmitry A. Abanin² and Zlatko Papić³✉

Thermalization is the inevitable fate of many complex quantum systems, whose dynamics allow them to fully explore the vast configuration space regardless of the initial state—the behaviour known as quantum ergodicity. In a quest for experimental realizations of coherent long-time dynamics, efforts have focused on ergodicity-breaking mechanisms, such as integrability and localization. The recent discovery of persistent revivals in quantum simulators based on Rydberg atoms have pointed to the existence of a new type of behaviour where the system rapidly relaxes for most initial conditions, while certain initial states give rise to non-ergodic dynamics. This collective effect has been named ‘quantum many-body scarring’ by analogy with a related form of weak ergodicity breaking that occurs for a single particle inside a stadium billiard potential. In this Review, we provide a pedagogical introduction to quantum many-body scars and highlight the emerging connections with the semiclassical quantization of many-body systems. We discuss the relation between scars and more general routes towards weak violations of ergodicity due to embedded algebras and non-thermal eigenstates, and highlight possible applications of scars in quantum technology.

A fundamental challenge in physics is to predict how systems evolve in time when taken out of their equilibrium state. Some familiar classical systems such as a clock pendulum have behaviour that is perfectly periodic and thus possible to predict at late times. This is an example of integrable behaviour. Integrable systems, however, are special; under perturbations, their periodic behaviour gradually disappears and ultimately gives way to chaos. The microscopic chaotic motion allows an ensemble of coupled systems to reach the state of thermal equilibrium, which can be effectively described using the textbook methods of statistical mechanics.

While many open questions remain in the field of classical chaotic systems, non-equilibrium quantum matter is another frontier of modern research. The intense focus on understanding routes to thermal equilibrium in isolated quantum systems with many degrees of freedom is partly due to the advent of synthetic systems based on atoms, ions or superconducting circuits as elementary building blocks^{1,2}. The relaxation times of these systems are long compared with those in traditional condensed-matter systems such as electrons in solids, and experiments allow monitoring of quantum dynamics at the single-atom level, thus opening a window to non-equilibrium quantum phenomena. These capabilities have renewed the interest in foundational questions of quantum physics, such as the emergence of a statistical-mechanics description in an isolated many-body system. Provided parts of the system are able to act as heat reservoirs for its other parts, an initial non-equilibrium state relaxes to thermal equilibrium, with a well-defined effective temperature. Such systems are called thermal or quantum ergodic.

Surprisingly, not all quantum systems are ergodic. For example, finely tuned one-dimensional (1D) systems³ may fail to thermalize owing to their rich symmetry structure, known as quantum integrability. However, when such systems are weakly perturbed, ergodicity is restored. On the other hand, disorder in an interacting system may induce many-body localization^{4,5}—a close relative of the celebrated Anderson localization for non-interacting particles. Similar to integrable systems, many-body localized systems have an

extensive number of conservation laws, which prevent thermalization. These conservation laws, however, are robust with respect to perturbations, and a many-body localized state is an example of a phase of matter that embodies strong ergodicity breaking.

The behaviour of quantum ergodic systems is governed by the eigenstate thermalization hypothesis (ETH)^{6,7}, a powerful conjecture, which explains the process of thermalization at the level of the system’s energy eigenstates. The ETH states that individual eigenstates of quantum ergodic systems act as thermal ensembles, and thus the system’s relaxation does not depend strongly on the initial conditions. However, in 2018, an experiment on a new family of Rydberg-atom quantum simulators revealed unforeseen dynamical behaviour⁸. The experiment observed significant qualitative differences in the dynamics, depending on the choice of the initial state: although certain initial states showed the relaxation to thermal ensembles that is expected in an ergodic system, other states exhibited periodic revivals. Such revivals were surprising given that the system did not have any conserved quantities other than total energy and it was free of disorder, thus ruling out integrability and localization as possible explanations. What made a particular initial state find its way back in the enormous Hilbert space of the 51-atom experimental system with dimension in excess of 4×10^{10} ?

A flurry of theoretical work has addressed the puzzle posed by the experiment: the nature and origin of this new regime of ergodicity breaking that is intermediate between thermalization and strong ergodicity breaking. The key to understanding this behaviour was the discovery of anomalous, non-thermal eigenstates in the highly excited energy spectrum of the Rydberg-atom system⁹. These eigenstates provide an example of what we will refer to as weak violation of the ETH: despite being strongly non-thermal, the anomalous eigenstates comprise a vanishing fraction of the Hilbert space, and they are immersed in a much larger sea of thermal eigenstates.

One may be puzzled as to why non-thermal eigenstates in the highly excited spectrum would have any importance. After all, the energy level spacing between highly excited eigenstates in a many-body system decreases exponentially with the number of

¹IST Austria, Klosterneuburg, Austria. ²Department of Theoretical Physics, University of Geneva, Geneva, Switzerland. ³School of Physics and Astronomy, University of Leeds, Leeds, UK. ✉e-mail: z.papic@leeds.ac.uk

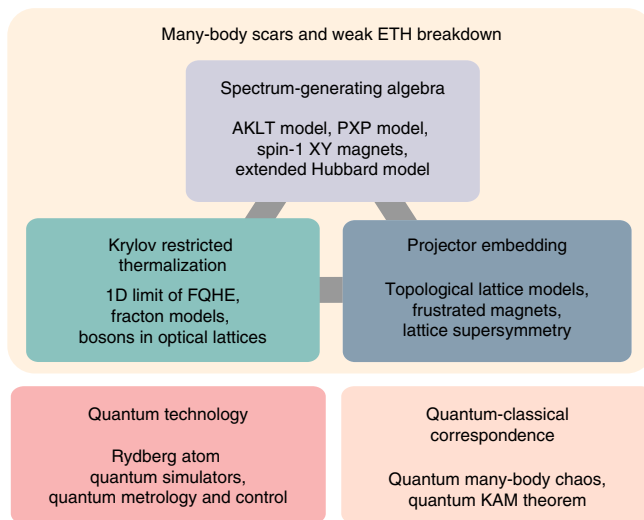


Fig. 1 | Origins and applications of weak ergodicity breaking. Top: examples of physical systems in which weak ergodicity breakdown has recently been discovered. These systems can be classified according to three main mechanisms of many-body scarring, reviewed in the text. Bottom: studies of many-body scarring have sparked interest in fundamental problems in the field of quantum many-body chaos and potential applications in quantum technology. FQHE, fractional quantum Hall effect.

atoms, and preparing the system in a particular eigenstate is challenging, if not impossible. Therefore, such eigenstates might be expected to remain ‘invisible’ to any experiment performed in the laboratory. Nevertheless, it was shown that these non-thermal eigenstates do indeed underpin the real-time dynamics observed in experiment, inspiring new connections between quantum many-body dynamics and studies of classical chaos¹⁰. By analogy with chaotic stadium billiards, which also host non-thermal eigenstates whose ergodicity breaking has been visualized as ‘scars’ of classical periodic orbits¹¹, the non-thermal eigenstates in the Rydberg-atom chains have been dubbed ‘quantum many-body scars’.

The discovery of quantum many-body scars has triggered broader investigations of weak ergodicity breaking in a variety of quantum systems, as opposed to the strong ergodicity breaking by integrability and disorder. These studies have unearthed a rich landscape of many-body scarred models with universal algebraic structures, shedding new light on a number of well-known condensed-matter models. In particular, the independently discovered non-thermal eigenstates in the Hubbard model and the Affleck–Kennedy–Lieb–Tasaki (AKLT) model were realized a posteriori to be examples of the same quantum many-body scar phenomena.

In this Review, we survey recent progress in weak ergodicity-breaking phenomena by highlighting relations between different realizations of non-thermal dynamics, schematically shown in Fig. 1. As we explain in detail below, known scarred models are characterized by a subspace that is decoupled from the rest of the energy spectrum and cannot be attributed to a symmetry of the system. The origin of this subspace can vary depending on the model, and a few common mechanisms, highlighted in Fig. 1, will be presented below. Furthermore, we discuss theoretical approaches that aim to bridge quantum and classical chaos in many-body systems, and the representation of scarred dynamics in terms of tensor networks. Finally, we outline promising future directions, putting an emphasis on emerging connections between weak ergodicity breaking and other fields. We mention other routes to weak ergodicity breaking, such as mesons in theories with confinement, the effects of additional conservation laws that fracture the Hilbert space, and frustration-driven glassy behaviour, whose relation to quantum

many-body scars remains to be fully understood. We conclude with a brief discussion of potential applications of quantum many-body scars in quantum sensing and metrology.

Phenomenology of quantum scarring

In experiments, quantum thermalization is conveniently probed by quenching the system: one prepares a non-equilibrium initial state $|\psi_0\rangle$, which is typically short-range correlated (for instance, a product state of particles), and monitors its fate after time t . For cold atoms and trapped ions, which are well isolated from any thermal bath, the system can be assumed to evolve according to the Schrödinger equation for the system’s Hamiltonian H . The process of thermalization is monitored by measuring the time evolution of local observables as the dynamics explores progressively larger parts of the system’s energy spectrum. The results of such measurements are remarkably different in typical quantum ergodic systems compared with non-ergodic localized systems. In ergodic systems, following a brief initial transient, local observables relax to their thermal value and stay near that value at later times. This behaviour is reminiscent of classical chaotic systems, which effectively ‘forget’ their initial condition. In contrast, in many-body localized systems, local observables reach a stationary value that is non-thermal, retaining the memory of the initial state—a hallmark of broken ergodicity.

It is important to emphasize that the dynamical behaviour of ergodic or non-ergodic systems mentioned above has been verified to hold for quenches from any physical initial states. This typicality was recently found to break down in experiments on arrays of Rydberg atoms⁸. The building block of these experiments is an individual Rydberg atom, which may be viewed as an effective two-level system in which the two states $|\circ\rangle$ and $|\bullet\rangle$ correspond, respectively, to an atom in the ground state and an atom in the so-called Rydberg state. When exposed to a microwave field, each atom undergoes Rabi oscillations, $|\circ\rangle \leftrightarrow |\bullet\rangle$, freely flipping between its two states. However, when assembled in an array, the atoms in $|\bullet\rangle$ state interact via repulsive van der Waals force, whose strength is strongly dependent on the distance between the atoms. By tuning the inter-atom distance, one can achieve the regime of the Rydberg blockade¹² where the excitations of neighbouring atoms, for example, $|\cdots\bullet\bullet\cdots\rangle$, are energetically prohibited. This makes the system kinetically constrained, as each atom is only allowed to flip if all of its neighbours are in the $|\circ\rangle$ state.

The dynamics of large 1D arrays of Rydberg atoms has been probed by studying quenches from a period-2 density-wave initial state, $|\mathbb{Z}_2\rangle \equiv |\bullet\circ\bullet\circ\cdots\rangle$, which is the state containing the maximal possible number of Rydberg excitations allowed by the blockade. The dynamics of domain-wall density, where domain walls are defined as adjacent $|\circ\circ\rangle$ or $|\bullet\bullet\rangle$ configurations (the latter is excluded in the regime of perfect blockade), revealed long-time oscillations (Fig. 2a). Such robust oscillations were surprising, given that the state $|\mathbb{Z}_2\rangle$ is not a low-energy state but rather corresponds to an infinite-temperature ensemble for the atoms in the Rydberg blockade. Thus the quench dynamics is not a priori limited to a small part of the energy spectrum and cannot be attributed to weakly interacting low-energy excitations in the system. Moreover, the oscillations could not be explained by any known conservation law in the system, and their frequency did not coincide with the bare Rabi frequency, signalling the importance of many-body effects.

The experimental findings have been corroborated by theoretical studies of an idealized model of atoms in the Rydberg blockade—the ‘PXP’ model¹³:

$$H_{\text{PXP}} = \sum_i P_{i-1} \sigma_i^x P_{i+1}. \quad (1)$$

Here $\sigma_i^x = |\circ\rangle_i \langle\bullet|_i + |\bullet\rangle_i \langle\circ|_i$ denotes the Pauli x matrix responsible for Rabi oscillations of an individual atom on site i , and projectors

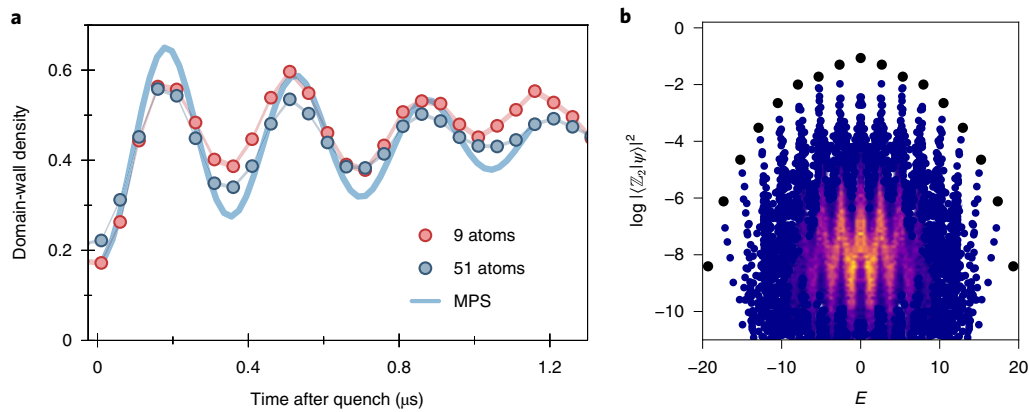


Fig. 2 | Weak breakdown of thermalization. **a**, Observation of persistent revivals in the domain-wall density when Rydberg-atom quantum simulators are quenched from the $|\mathbb{Z}_2\rangle$ initial state⁸. The oscillations were found to persist in large chains up to 51 atoms, and they were reproduced in dynamical simulations using matrix product state methods. **b**, Weak breakdown of thermalization in Rydberg-atom arrays was theoretically attributed to atypical eigenstates—quantum many-body scars—which are distinguished by their anomalously enhanced overlaps with the $|\mathbb{Z}_2\rangle$ state⁹. Each dot represents an eigenstate of energy E in the PXP model in equation (1) with $L=32$ atoms. The colour scheme illustrates the density of points. Panel **a** reproduced with permission from ref. ⁸, Springer Nature Ltd. Panel **b** adapted with permission from ref. ⁹, Springer Nature Ltd.

onto the ground state, $P_i = |\circ\rangle_i\langle\circ|_i$, enforce the Rydberg blockade and make the model interacting. Numerical studies have observed that the PXP energy levels repel, thus confirming that the model is non-integrable⁹. Further, simulations of the quench dynamics have demonstrated revivals of the wavefunction and local observables when the system is quenched from the $|\mathbb{Z}_2\rangle$ state^{14,15}, as well as the period-3 density-wave state $|\mathbb{Z}_3\rangle \equiv |\bullet\circ\circ\bullet\circ\circ\dots\rangle$. In contrast, other initial states, such as the $|0\rangle = |\circ\circ\circ\dots\rangle$ state and the period-4 density-wave state, showed fast relaxation without revivals¹⁶. Similar phenomenology has also been identified in the 2D PXP model^{17,18}, and in related models of transverse Ising ladders¹⁹ and the periodically driven PXP model^{20–22}. This special behaviour of the PXP model was found to be in general destroyed by perturbations, which can make this model integrable²³, frustration free²⁴ or thermalizing¹⁶, although a certain degree of robustness was demonstrated with respect to disorder²⁵. Moreover, it was argued that for weak perturbations, the dynamical signatures of scars survive for parametrically long times²⁶.

An important step in understanding the origin of the observed oscillations was made by theoretical studies of many-body eigenstates of the PXP model. Figure 2b reveals a number of ‘atypical’ eigenstates in the spectrum of the PXP model, which are distinguished by their high overlap with the same $|\mathbb{Z}_2\rangle$ state used for initiating the quench in Fig. 2a. For a quantum ergodic system, the ETH stipulates that these overlaps should be a smooth function of energy; by contrast, the strong enhancement of overlaps of certain eigenstates compared with others at the same energy E , seen in Fig. 2b, signals a breakdown of the ETH. This is a weak violation of the ETH since the number of special eigenstates was found to scale linearly with the number of atoms, in contrast to an exponentially larger number of thermalizing eigenstates. Moreover, the special eigenstates are ‘embedded’ at roughly equidistant energies in an otherwise thermalizing spectrum of the PXP model, thus accounting for the dynamical revivals in Fig. 2a with a single dominant frequency. We note that various schemes for constructing some of these atypical eigenstates in the PXP model, both exact²⁷ and approximate^{16,28}, have been devised.

The core phenomenology of the PXP model—the small number of ETH-violating eigenstates within the thermalizing spectrum, and the presence of many-body revivals and slow relaxation in quenches from specific initial states—bears parallels with the physics of a single particle confined to a stadium-shaped billiard. In the latter case, the dynamics of a quantum wave packet is known to be

sensitive to the initial conditions, which was attributed to the existence of unstable periodic orbits when the billiard is made classical by sending $\hbar \rightarrow 0$ (Box 1). Initialization of a quantum wave packet on or near such an orbit leads to dynamical recurrences in which the particle tends to cluster around the orbit, a phenomenon called quantum scarring¹¹. Moreover, the periodic orbit leaves an imprint on the eigenfunctions of a particle, which exhibit anomalous concentration in the vicinity of the periodic orbit, rather than being spread uniformly across the billiard.

While the analogy between revivals in the PXP model and scars in billiards is indeed suggestive, making it more precise has required new theoretical insights. As we discuss below, these approaches have followed two complementary strands. The first approach, discussed in the section ‘Mechanisms of weak ergodicity breaking’, focuses on constructing non-thermal eigenstates in many-body quantum systems. This approach has been particularly fruitful in identifying a large family of scarred many-body systems, some of which were highlighted in Fig. 1. An alternative perspective, which focuses on parallels between quantum many-body dynamics and classical dynamical systems, will be discussed in the section ‘Scars and periodic orbits in many-body systems’.

Mechanisms of weak ergodicity breaking

Recent theoretical studies have identified non-thermal eigenstates in a plethora of non-integrable quantum models. A common trait of all these models is the emergence of a decoupled subspace within the many-body Hilbert space, in general without any underlying symmetry, spanned by the non-thermal eigenstates. Formally, the Hamiltonian of such systems effectively decomposes into a block-diagonal form

$$H \approx H_{\text{scar}} \oplus H_{\text{thermal}}, \quad (2)$$

where H_{scar} is the block of the Hamiltonian acting on a scarred subspace which is (approximately, or even exactly) decoupled from the thermalizing subspace. The eigenstates that inhabit the scarred subspace where H_{scar} operates violate the ETH and have different properties from the much larger number of thermal eigenstates of H_{thermal} . Below, we elucidate and contrast three mechanisms that lead to such a decoupled subspace, corresponding to the three scenarios presented in Fig. 3. These mechanisms are realized by diverse physical systems (Fig. 4).

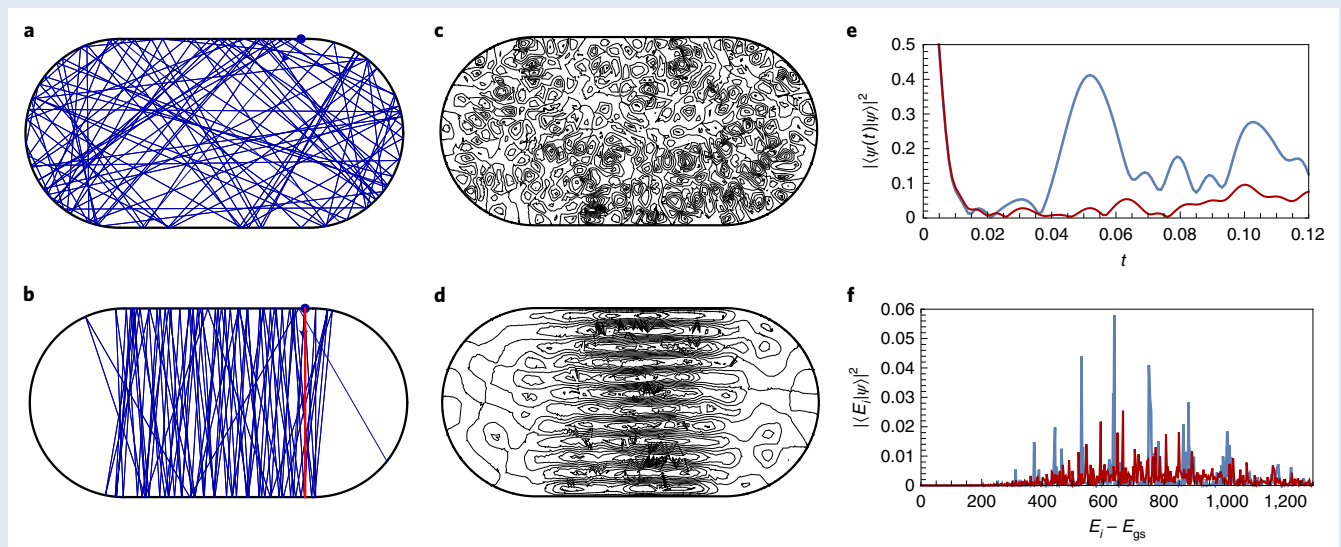
Box 1 | Scars in quantum billiards

What can we learn about the behaviour of a quantum system by looking at its classical counterpart? Bohr–Sommerfeld quantization demonstrates that classical integrable systems, such as the harmonic oscillator or hydrogen atom, have very special quantum spectrum and eigenstates. For classically chaotic systems, such as the Bunimovich stadium in the figure here, this quantization method does not work. Typically, quantum counterparts of classically chaotic systems display level repulsion in their spectrum, and their eigenstates look random. However, short periodic orbits may leave a strong imprint on the system’s quantum dynamics and eigenstate properties—this effect is called ‘quantum scarring’¹⁰¹. An example of such an orbit is the marginally stable, ‘bouncing ball’ trajectory in panel **b** for which scarring can be rigorously proven; more strikingly, there is numerical evidence of scarring in certain unstable periodic orbits¹¹. Scarring is a weak form of ergodicity breaking since the individual eigenstates of the billiard are ‘almost always’ ergodic as the phase space area affected by scarring vanishes in the limit $\hbar \rightarrow 0$, shrinking around the orbit.

How does one detect scars? Most simply, by visualizing the wavefunction probability density, as in the case of the Bunimovich

stadium in panels **c** and **d**. The probability density can be directly compared with the corresponding classical orbits in panels **a** and **b**. Moreover, scars leave an imprint on the dynamics: a wave packet launched in the vicinity of a periodic orbit will tend to cluster around the orbit at later times, displaying larger return probability than a wave packet launched elsewhere in phase space. This is seen in the autocorrelation function in panel **e**. Furthermore, such a wave packet can be expanded over a small number of eigenstates that have approximately similar energy spacing (panel **f**), in contrast to an arbitrary wave packet.

What is the significance of quantum scars? First, scars provide a counterexample to the intuitive expectation that every eigenstate of a classically chaotic system should locally look like a random superposition of plane waves¹⁰². Second, also counterintuitively, a scarred quantum system appears more ‘regular’ than its classical counterpart, since in the latter case there is no enhancement of density along the periodic orbit in the long-time limit. Finally, scars play a role in many experiments, including microwave cavities¹⁰³, semiconductor quantum wells¹⁰⁴ and the hydrogen atom in a magnetic field¹⁰⁵.



Scars in a stadium billiard. **a**, A classical particle initialized away from a periodic trajectory displays chaotic motion. **b**, In contrast, when launched near a ‘bouncing ball’ trajectory (shown in red), the particle spends a long time in its vicinity before escaping. **c**, The probability density of a typical highly excited eigenstate of the billiard resembles a collection of random plane waves. **d**, The probability density of a quantum-scarred eigenstate looks very different from a collection of plane waves, instead being strongly concentrated near the periodic trajectory. The eigenstates of the billiard are obtained by solving the Schrödinger equation with the wavefunction vanishing at the boundary. **e, f**, Autocorrelation function of a Gaussian wave packet launched vertically at the centre of the billiard shows pronounced revivals (blue line, **e**), and the expansion of the initial state over the billiard eigenstates reveals a periodic sequence of peaks (blue line, **f**). In contrast, a wave packet launched at a 45° angle does not revive and features a continuum of frequencies (red lines). E_i is the energy of the i th eigenstate and E_{gs} is the energy of the ground state.

Spectrum-generating algebra. Highly excited non-thermal eigenstates can be constructed systematically using the ‘spectrum-generating algebras’ originally introduced in the context of high-energy physics²⁹ and subsequently applied to the Hubbard model^{30,31}. The first exact construction of many-body scarred eigenstates using this method was achieved in the AKLT³², extending earlier work in ref. ³³.

A spectrum-generating algebra is defined by a local operator \hat{Q}^\dagger that obeys $([H, \hat{Q}^\dagger] - \omega \hat{Q}^\dagger)W = 0$, where ω is some energy scale

and W is a linear subspace of the full Hilbert space and invariant under \hat{Q}^\dagger . Many-body scarring occurs when W is a subset of the entire Hilbert space and \hat{Q}^\dagger is not associated with a symmetry of the Hamiltonian. Then, starting from some eigenstate $|\psi_0\rangle$ of H that belongs to the subspace W , the tower of states, $(\hat{Q}^\dagger)^n |\psi_0\rangle$, are all eigenstates of H with energies $E_0 + n\omega$, where n is an integer or zero. The eigenstates $(\hat{Q}^\dagger)^n |\psi_0\rangle$ are many-body scars because their properties can be strongly non-thermal, assuming $|\psi_0\rangle$ is sufficiently ‘simple’ (for instance, the ground state of H if the latter

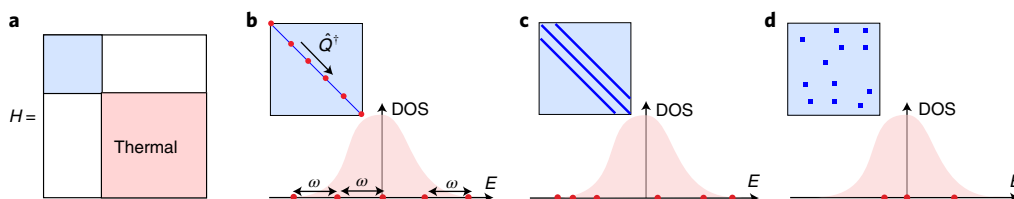


Fig. 3 | Embeddings of scarred eigenstates in a many-body system. **a**, The Hamiltonian matrix H , acting on the full Hilbert space, is schematically split into the non-ergodic subspace (blue box) and the remaining thermal subspace (red box). **b–d**, Possible mechanisms underlying the emergence of the decoupled subspace. Density of states (DOS) schematically shows the positions of scarred eigenstates (red dots) within the continuum of thermalizing states. **b**, Exact scars due to a spectrum-generating algebra, and the resulting eigenstates which are equidistant in energy. **c**, Exact Krylov subspace represented by a tridiagonal matrix. **d**, General subspace resulting from projector embedding. In any of these cases, the scarred subspace, like in the PXX model, need not be exactly decoupled from the thermalizing bulk.

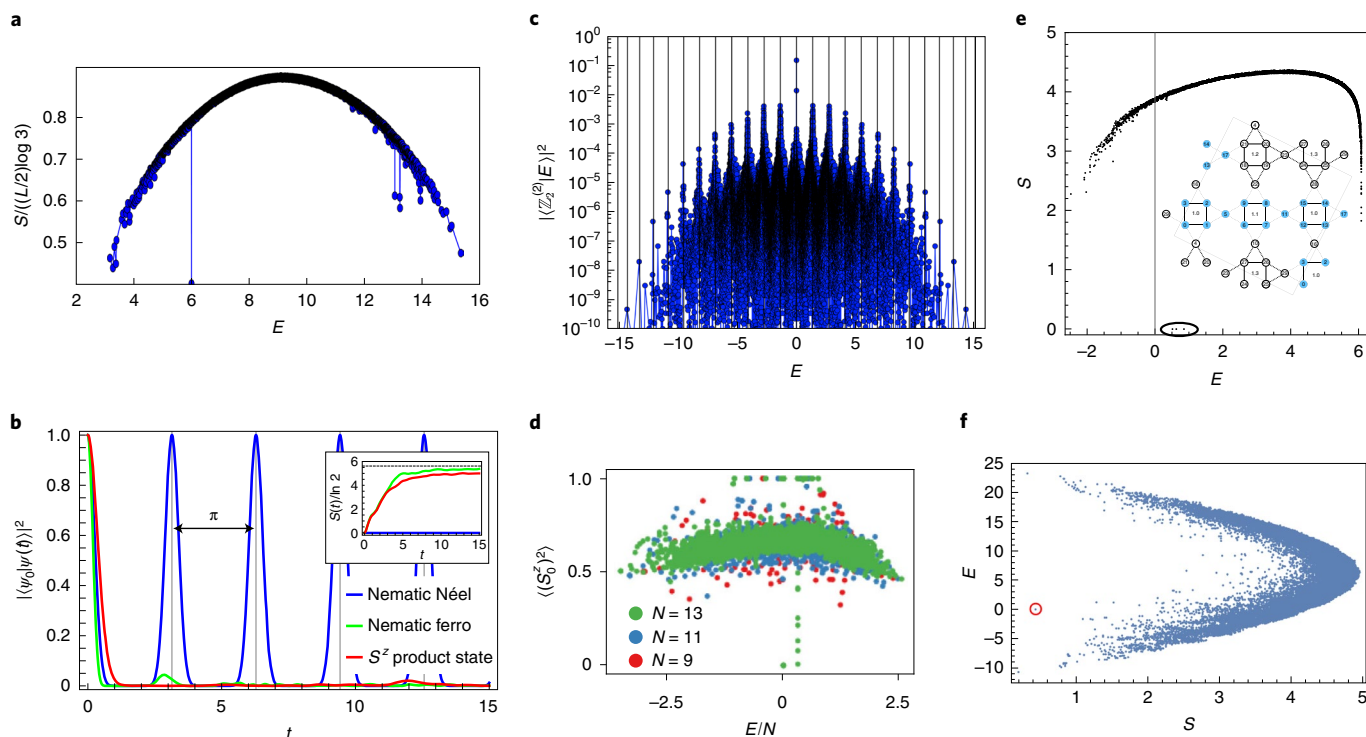


Fig. 4 | Mechanisms and physical realizations of weak ergodicity breaking. **a, b**, Many-body scars due to spectrum-generating algebras. **a**, Exact scars in the AKLT model distinguished by their low entanglement entropy S (ref. ³²). L , system size. **b**, Perfect fidelity revival due to exact scars in a spin-1 XY magnet³⁹. The inset shows the growth of entanglement entropy following a quench from the initial states denoted in the legend of the main panel. **c, d**, Krylov subspaces in fracton-like models. The model of the fractional quantum Hall effect on a thin cylinder⁵⁴ supports scarred eigenstates and revivals from a product state (**c**), while local observables in a spin-1 model with dipole conservation symmetry⁵⁷ weakly violate the ETH (**d**). **e, f**, Projector embedding of scarred states into thermalizing spectra. **e**, Geometrical frustration on a 2D square-kagome network (inset) allows embedding of weakly entangled states of localized magnons (circled)⁶³. **f**, Stochastic deformations of topological models, such as the 1D cluster model, allow embedding of scarred states (circled)⁶⁵. The same method applies to 2D toric code and 3D X-cube models. Panels adapted with permission from: **a**, ref. ³², APS; **b**, ref. ³⁹, APS; **e**, ref. ⁶³ under a Creative Commons licence CC BY 4.0. Panels reproduced with permission from: **c**, ref. ⁵⁴, APS; **d**, ref. ⁵⁷ under a Creative Commons licence CC BY 4.0; **f**, ref. ⁶⁵ under a Creative Commons licence CC BY 4.0.

is gapped) and \hat{Q}^\dagger is a local operator (such as a sum of on-site spin flips in quantum spin chain models).

In many cases, \hat{Q}^\dagger has a physical interpretation of creating a quasiparticle excitation (for example, a magnon) such that repeated applications of \hat{Q}^\dagger create a condensate of such quasiparticles. In a class of frustration-free models that includes the AKLT model³⁴, the quasiparticle condensates are exact eigenstates with finite energy density, thus violating the ETH. A convenient diagnostic for ETH violation and identifying scarred eigenstates is the entanglement entropy S , that is, the von Neumann entropy of a

given eigenstate’s reduced density matrix describing a subsystem of the full system. In ETH systems, the entanglement entropy of eigenstates scales extensively with the size of the subsystem. By contrast, scarred eigenstates have entanglement that increases only logarithmically with system size. This property means they can be detected as entropy outliers among the majority of eigenstates with volume-law entanglement, as seen in Fig. 4a for the AKLT model. Another important clue when looking for scarred eigenstates is that they appear at energies that are rational multiples of ω .

In related approaches, a tower of scarred eigenstates can be ‘engineered’ by starting with a \hat{Q}^\dagger that defines a symmetry of H , and the subspace W coincides with the full Hilbert space. Adding a suitable perturbation that breaks this symmetry, while at the same time annihilates the tower $(\hat{Q}^\dagger)^n |\psi_0\rangle$, leaves the states in the tower as true many-body scars in the perturbed model³⁵. For example, in the Hubbard model, \hat{Q}^\dagger plays the role of an SU(2) ‘eta pairing’ symmetry³⁶, which is broken in the extended Hubbard model and gives way to many-body scars^{37,38}. A similar construction holds in a spin-1 XY magnet³⁹, which also hosts perfect wavefunction revivals from certain easily prepared initial states, as illustrated by its quantum fidelity, $|\langle \psi_0 | \psi(t) \rangle|^2$, in Fig. 4b. Further variations of the algebraic construction have been given for spin-1 magnets⁴⁰, a spin-1/2 model with emergent kinetic constraints⁴¹, a spin chain with the dynamical Onsager algebra⁴² and a 2D frustrated spin-1/2 kagome antiferromagnet⁴³. Recent results have provided a more general framework for the construction of non-thermalizing subspaces using group theory^{44–46}. It has also been pointed out that spectrum-generating algebra can arise in open quantum systems, for example, in the presence of dissipation or periodic driving^{47,48}.

Finally, the PXP model in equation (1) also realizes an embedded algebra, in this case an approximate SU(2) spin algebra⁴⁹. The spin raising operator H^+ creates a Rydberg excitation anywhere on the even sublattice and removes an excitation anywhere on the odd sublattice, while respecting the Rydberg constraint. Similarly, the spin lowering operator H^- performs the same process with the sublattices exchanged. The reason for this choice of H^\pm is that their commutator defines the z -projection of spin, $H^z \equiv \frac{1}{2}[H^+, H^-]$, for which $|\mathbb{Z}_2\rangle$ plays the role of the extremal weight state. In principle, using this construction, one could form the Casimir operator for the SU(2) algebra and obtain the tower of non-thermal eigenstates by acting repeatedly with H^+ on the ground state of the Casimir, mirroring the general procedure outlined previously. This procedure is not analytically tractable, because the ground state of the Casimir operator is not known and the algebra of the PXP model is only approximate (however, recent work has shown that weak deformations of the PXP model make the algebra and dynamical revivals progressively more accurate^{49–51}). Instead, different schemes have been used to approximate scarred eigenstates in the PXP model starting from the $|\mathbb{Z}_2\rangle$ product state^{16,52}.

Krylov restricted thermalization. The spectrum-generating algebra approach relies on the tower operator \hat{Q}^\dagger to construct the non-thermalizing subspace. In practice, finding such operators is likely to be limited to cases where they can be expressed in a simple local form. We next describe a related mechanism for producing exactly embedded subspaces, which does not require a priori knowledge of \hat{Q}^\dagger .

For a Hamiltonian H and some arbitrary vector in the Hilbert space, $|\psi_0\rangle$, the Krylov subspace, \mathcal{K} , is defined as a set of all vectors obtained by repeated action of H on $|\psi_0\rangle$, that is, $\mathcal{K} = \text{span}\{|\psi_0\rangle, H|\psi_0\rangle, H^2|\psi_0\rangle, \dots\}$. In numerical linear algebra, subspace \mathcal{K} is routinely used in iterative methods for finding extremal eigenvalues of a large matrix H , such as the Arnoldi and Lanczos algorithms. A special case of particular interest is when \mathcal{K} happens to be finite because the sequence of Krylov vectors terminates after $n+1$ steps: $H^{n+1}|\psi_0\rangle = 0$. This causes a dynamical ‘fracture’ of the Hilbert space in the sense that the Schrödinger dynamics initialized in any state $|\psi\rangle \in \mathcal{K}$ must remain within the same subspace at any later time, $\exp(-\frac{i}{\hbar}tH)|\psi\rangle \in \mathcal{K}$, hence the name ‘Krylov restricted thermalization’⁵³. Note that \mathcal{K} can be as small as a single vector or exponentially large in system size, and it can be either integrable or thermalizing. By performing a Gram–Schmidt orthogonalization, we can transform \mathcal{K} into a tridiagonal matrix, which will be perfectly decoupled from the rest of the spectrum of H . We distinguish the case of the Krylov subspace from the previous case of the algebra

subspace because, in general, it can be difficult to analytically diagonalize the tridiagonal matrix and construct the corresponding \hat{Q}^\dagger . Note that a tridiagonal Krylov subspace does not guarantee revivals, even if the root state $|\psi_0\rangle$ is experimentally preparable. This is because general tridiagonal matrices do not support revivals, unless their matrix elements are tuned to special values. Moreover, depending on the model, the Krylov subspace may only be approximately decoupled, so that there may exist small matrix elements that connect it with the thermalizing bulk.

Realizations of Krylov subspaces occur in models of the fractional quantum Hall effect in a quasi-1D limit⁵⁴ and in models of bosons with constrained hopping on optical lattices^{55,56}. In the former case, shown in Fig. 4c, \mathcal{K} is thermalizing but also supports scarred eigenstates and revivals from a particular density-wave product state. Scarred towers in overlaps with a density-wave state in Fig. 4c signal a weak ETH violation due to anomalous concentration of eigenstates in the Hilbert space, analogous to the case of the PXP model in Fig. 2b.

More generally, the Krylov fracture was shown to be present in both Hamiltonian models⁵⁷ and random-circuit models^{58,59} that feature conservation of dipole moments—a symmetry that is characteristic of the so-called fracton topological phases. An example of weak breaking of the ETH in a 1D fracton-like model⁵⁷ is shown in Fig. 4d, which shows the matrix elements of a local spin observable in the system’s eigenstates. Once again, the large spread of these matrix elements and their non-monotonic behaviour as a function of energy indicate a weak violation of the ETH.

Projector embedding. At the highest level of abstraction, we can ask if one could embed an arbitrary subspace into the spectrum of a thermalizing system. This question had been independently explored by Shiraishi and Mori⁶⁰ in the context of systematic violations of strong ETH. More recently, the same ‘projector embedding’ approach has turned out to be a fruitful method for constructing many-body scarred states in diverse models ranging from lattice supersymmetry⁶¹ to flat bands⁶².

For concreteness, assume we are given a certain set of states $|\psi_i\rangle$ that span our target scar subspace $H_{\text{scar}} = \text{span}\{|\psi_i\rangle\}$, which we wish to embed into a thermalizing Hamiltonian H as in equation (2). Projector embedding assumes that our target states $|\psi_i\rangle$, being non-thermal, are annihilated by local projectors, $P_i|\psi_j\rangle = 0$, for any i ranging over lattice sites $1, 2, \dots, L$. Next, consider a lattice Hamiltonian of the form $H = \sum_{i=1}^L P_i h_i P_i + H'$, where h_i are arbitrary operators that have support on a finite number of sites around i , and $[H', P_i] = 0$ for all i . It follows that $P_i H |\psi_j\rangle = P_i H' |\psi_j\rangle = H' P_i |\psi_j\rangle = 0$, such that the subspace spanned by $|\psi_i\rangle$ is closed under the action of H . Therefore, H takes the desired block-diagonal form in equation (2). The target eigenstates can, in principle, be embedded at arbitrarily high energies for a suitably chosen h_i and H' , which also ensures that the model is overall non-integrable⁶⁰. However, there is no guarantee that the embedded states will be equidistant in energy, and they may even be degenerate, such that this scheme could produce models that do not exhibit wavefunction revivals.

Physical mechanisms such as geometrical frustration in correlated materials can implement the projector embedding. Figure 4e shows an example of a 2D square-kagome lattice model, where scarred states representing localized magnons can be embedded into the highly excited energy spectrum⁶³. Moreover, projector embedding naturally lends itself to physical realization in various topologically ordered lattice models⁶⁴, which are themselves defined in terms of projectors. Stochastic deformations of such models⁶⁵, which include the 2D toric code model and 3D X-cube model, can be used to embed scarred states, as shown in Fig. 4f.

In summary, we have presented three mechanisms that can give rise to non-thermal eigenstates in the spectrum of an otherwise thermalizing model. We emphasize that these mechanisms

are not mutually exclusive; rather, they underscore how weak ergodicity breaking is manifested in various models. The connections between different mechanisms are most saliently illustrated by the PXP model. The PXP model, with its generalizations to higher spins¹⁰ and quantum clock models⁶⁶, falls into the category of spectrum-generating algebras, yet its algebra is only approximate, and the subspace has weak couplings to the thermal bulk. In addition, the PXP model also realizes an approximate Krylov subspace built upon the $|\mathbb{Z}_2\rangle$ state (the subspace becomes exact when generated by H^+). Finally, a single PXP eigenstate at zero energy in the middle of the spectrum can be viewed as a projector-embedded AKLT ground state⁶⁷. While similar connections between scarring mechanisms may be anticipated in other models mentioned above, their demonstration remains an open problem.

Scars and periodic orbits in many-body systems

The term ‘quantum many-body scar’ is nowadays commonly used to denote general non-thermal eigenstates embedded in the spectra of non-integrable systems like the ones that we surveyed above. However, to justify the analogy with scars in quantum billiards, there should exist some notion of a classical trajectory underlying the non-thermal eigenstates. Finding such a trajectory, and more generally the classical counterpart of a many-body quantum system, is indeed one of the central goals of the field of quantum chaos. However, two commonly used methods—mean-field theory and large- N limit—are not expected to work for the majority of quantum models discussed in the section ‘Mechanisms of weak ergodicity breaking’, as these models have a small on-site Hilbert space, so they are far away from the mean-field limit. Progress on this question has recently been achieved by using a variational framework based on states that allow entanglement to be incorporated, thus going beyond mean-field approaches. Below, we briefly outline this method and discuss the new physical insights it gives into the PXP model—the only available example at this stage. Afterwards, we discuss the prospects of finding periodic trajectories in other scarred models and broader applications of the method beyond many-body scars.

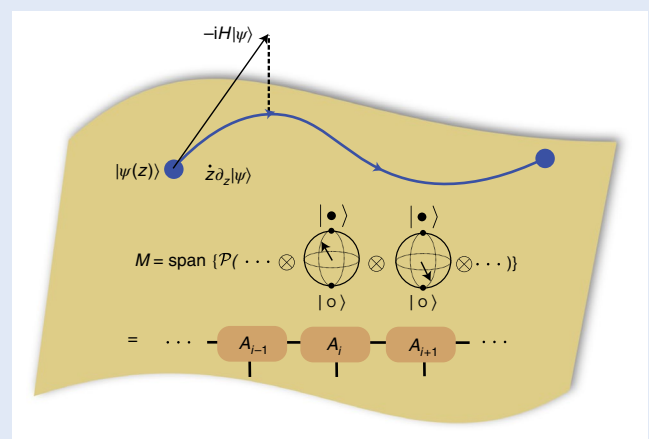
Optimal projection of quantum dynamics onto a given variational manifold can be achieved by the time-dependent variational principle (TDVP) pioneered by Dirac⁶⁸. The variational principle determines the best direction of evolution within the manifold, such that the difference between exact and projected dynamics is minimal (see Box 2 for details). TDVP has played an important role in studies of semiclassical dynamics⁶⁹, and in recent years it has been turned into a powerful computational tool for many-body systems by parametrizing the manifold via a family of the ‘matrix product states’ (MPS)⁷⁰. The advantage of MPS parametrization is that it naturally extends mean-field-like product states by incorporating non-trivial but finite range correlations. In particular, the results of unitary time evolution from the initial product state can be efficiently represented as an MPS state. This MPS framework has recently been extended into a path integral over ‘entanglement’-based degrees of freedom⁷¹, and it has been used to calculate the diffusion coefficient in quantum many-body systems⁷².

The ability of MPS states to incorporate entanglement made it an ideal tool to explore semiclassical dynamics of the PXP model, which involves non-local correlations due to the Rydberg blockade. The variational MPS approach is tailored to capture dynamics from the initial $|\mathbb{Z}_2\rangle$ state¹⁰. This state is a period-2 density wave, which can be described using a two-atom unit cell. The variational MPS state is parametrized by two angles, θ_o and θ_e , which describe the state of Rydberg atoms on odd and even sites, respectively, so that $(\theta_o, \theta_e) = (0, \pi)$ and $(\theta_o, \theta_e) = (\pi, 0)$ correspond to the $|\mathbb{Z}_2\rangle = |\bullet \circ \bullet \circ \dots\rangle$ product state and its partner shifted by one lattice site, $|\mathbb{Z}'_2\rangle = |\circ \bullet \circ \bullet \dots\rangle$. TDVP projection of dynamics on such MPS manifolds, discussed in Box 2, results in a system

Box 2 | Variational method for quantum many-body scars

Optimal projection of quantum dynamics onto a given variational manifold \mathcal{M} , parametrized as $|\psi(z)\rangle$, can be achieved by TDVP. The variational principle determines the best direction of evolution within the manifold, $\dot{z}\partial_z|\psi\rangle$, such that the difference between exact and projected dynamics is minimal, $\gamma^2 = |\dot{z}\partial_z|\psi\rangle + iH|\psi\rangle|^2$. The quantity γ^2 is called quantum leakage and quantifies the instantaneous disagreement between quantum dynamics and its projection. To capture quantum many-body dynamics, the manifold can be parametrized by MPS states, whose bond dimension controls the amount of entanglement generated during time evolution⁷⁰. The semiclassical dynamics emerges naturally in this approach by keeping the bond dimension of the MPS small, allowing to systematically go beyond the mean-field description.

While the TDVP approach can be applied to any quantum system, its application to the PXP model with MPS of bond dimension 2 results in a particularly elegant and analytically tractable classical dynamical system¹⁰. To describe coherent many-body oscillations in the PXP model, inspired by the mean-field picture, one may attempt to use the manifold of product states, $\dots(\cos\theta_e|\circ\rangle + \sin\theta_e|\bullet\rangle)(\cos\theta_o|\circ\rangle + \sin\theta_o|\bullet\rangle)\dots$, parametrized by two degrees of freedom—the angles θ_e and θ_o . These angles describe the state of atoms on even and odd sites in the chain. However, such a state violates the Rydberg blockade condition. Instead, the Rydberg constraint can be satisfied in the MPS manifold where one assigns the tensor $A^{|\bullet\rangle} = \sigma^+$ to the $|\bullet\rangle$ state. Property $A^{|\bullet\rangle}A^{|\bullet\rangle} = (\sigma^+)^2 = 0$ of Pauli raising operators $\sigma^+ = (\sigma^x + i\sigma^y)/2$ guarantees that the weight of configurations with any two adjacent states $|\bullet\bullet\rangle$ vanishes. Application of TDVP to such states results in the system of classical nonlinear differential equations for $\theta_{e,o}$. Such a mapping of quantum dynamics onto a classical dynamical system provides an alternative perspective on quantum many-body scars and establishes a close analogy to their classical counterparts (Box 1), in essence providing an alternative notion of a semiclassical limit. Finding suitable manifolds and extending this approach to dynamics in other models that have non-thermal eigenstates remains an outstanding open problem.



Variational method for quantum many-body scars. The time-dependent variational principle captures the optimal projection of quantum dynamics onto a given variational manifold. The studies of the PXP model use MPSs as a variational manifold, where each atom is described by a single angle. The presence of the Rydberg blockade, implemented by projector \mathcal{P} , results in entanglement, which requires that the MPS tensors A_i have a bond dimension of 2.

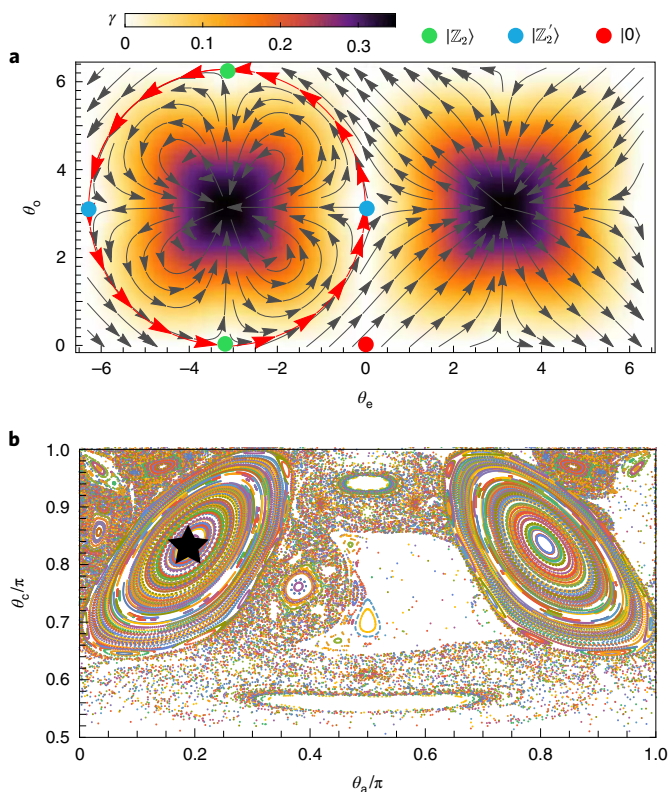


Fig. 5 | Many-body scarring and periodic orbits in semiclassical dynamics.

a, Phase diagram obtained from the variational ansatz with two degrees of freedom reveals an unstable periodic trajectory, which is responsible for the revivals in the PXP model from the $|\mathbb{Z}_2\rangle$ state¹⁰. Colour scale shows quantum leakage, which quantifies the instantaneous discrepancy between quantum and variational dynamics. **b**, Dynamical system with three angles $\theta_a, \theta_b, \theta_c$ results in a Poincaré section with many stable periodic trajectories (one of them denoted by the star) in centres of regular regions surrounded by the chaotic sea⁷³. This classical dynamical system describes behaviour such as quantum revivals from the $|\mathbb{Z}_3\rangle$ initial state in the PXP model. Panel **a** reproduced with permission from ref. ¹⁰, APS. Panel **b** adapted with permission from ref. ⁷³ under a Creative Commons licence CC BY 4.0.

of classical nonlinear equations that govern the evolution of the angles, $\partial_t \theta_{\alpha} = f(\theta_a, \theta_b, \theta_c)$. The resulting phase portrait in Fig. 5a reveals a periodic trajectory that passes through $|\mathbb{Z}_2\rangle$ and $|\mathbb{Z}'_2\rangle$ states, thereby explaining the revivals in the PXP model from a period-2 density-wave state. The ‘quantum leakage’ (Box 2) quantifies the discrepancy between quantum and variational dynamics and remains low in the vicinity of the classical trajectory in Fig. 5a, thus justifying the existence of revivals in the quantum evolution.

Finding the classical trajectory behind quantum revivals from $|\mathbb{Z}_2\rangle$ state provided a complementary picture behind weak ergodicity breaking by eigenstates of the PXP model. This variational approach was also extended to capture quantum dynamics for PXP model from more complicated initial states or in higher dimensions⁷³. In particular, an MPS variational ansatz with three angles $\theta_a, \theta_b, \theta_c$ was used to study dynamics from period-3 density-wave state, $|\mathbb{Z}_3\rangle = |\bullet \circ \circ \dots\rangle$. TDVP projection of quantum dynamics onto such an MPS manifold gave rise to a 3D dynamical system, whose Poincaré sections are shown in Fig. 5b. A prominent feature of this dynamical system was the existence of mixed phase space—the coexistence of classical chaotic regions with regions of stable motion, the so-called Kolmogorov–Arnold–Moser (KAM) tori⁷⁴. The KAM tori host stable periodic orbits in their centres (one such orbit is shown by the star in Fig. 5b). This provides a practical way of finding the

most non-ergodic initial state with period-3 translation invariance. Furthermore, one may expect that the robustness of classical KAM tori to weak deformations may be used to infer the stability of the corresponding quantum model to local perturbations. The mapping of quantum dynamics onto a classical dynamical system via TDVP suggests an intriguing direction for extending the KAM theorem to quantum systems, in a way that complements other recent attempts based on weakly broken quantum integrability⁷⁵.

The existence of classical periodic trajectories underlying quantum revivals in the PXP model calls for exploration of semiclassical dynamics in other scarred models discussed in ‘Mechanisms of weak ergodicity breaking’. Although the projector-based embedding scenario is, in general, unlikely to have underlying periodic trajectories, for models with a spectrum-generating algebra one could imagine constructing a variational subspace using properties of the \hat{Q} operator. Such a construction of classical periodic trajectories in a broader family of models could in principle be used as a finer classification scheme for models displaying weak ETH violation in their eigenstate properties.

Perspective

Recent studies of quantum many-body scars and related phenomena, described in this Review, have revealed a new kind of dynamical behaviour in many-body systems—weak ergodicity breaking. The defining feature of weak ergodicity breaking is strong dependence of relaxation dynamics on the system’s initial configuration. In contrast to conventional ergodic systems, certain many-body states are long-lived, exhibiting parametrically slow relaxation, as opposed to other initial configurations that thermalize quickly. These findings have pointed out that the ETH, in its strong form, does not apply to a large class of systems that host anomalous, non-thermal eigenstates, and exhibit long-time coherent dynamics.

The discovery of quantum many-body scars serves as a reminder that the understanding of thermalization and chaos in quantum many-body systems is far from complete and requires building a more elaborate theory and the accompanying methodological toolbox. The eigenstate description revealed a common pattern in different families of scarred systems—an emergent decoupled subspace within the full many-body Hilbert space. Although we have presented a few mechanisms that could underlie the existence of such a non-thermal subspace, it is desirable to build their complete classification and find robust diagnostics of quantum many-body scars beyond entanglement entropy. In particular, more work is needed to understand the precise connection between many-body scarring and two broad classes of weak ergodicity-breaking phenomena: theories with confinement^{76–80} and lattice gauge theories^{81–83}. The latter—in particular the 1D quantum link model that has recently been realized in a Bose–Hubbard quantum simulator⁸⁴—have intriguing connections with the PXP model⁸⁵, and it would be interesting to explore possible connections in higher dimensions⁸⁶. If accomplished, the classification of non-thermal subspaces could shed light on the physical mechanisms that lead to quantum many-body scars. Empirically, kinetically constrained systems seem to be especially likely to host quantum many-body scars; hence it would be important to understand the role of dynamical constraints that can lead to glassy-like dynamics^{87–91}.

More generally, the variational approach to scarred dynamics complements recent efforts in understanding parallels between classical chaos measures on the one hand, and thermalizing quantum dynamics and its underlying transport coefficients on the other hand^{72,92}. Although many-body scarred models are quantum chaotic, their properties deviate from other chaotic models such as the Sachdev–Ye–Kitaev (SYK) model^{93,94}, which has attracted much attention as the fastest scrambler of quantum information⁹⁵. Such deviations could be identified and studied more systematically using the variational approach and its resulting mixed phase

portraits, which appear to be a generic feature of local Hamiltonians. Armed with a better understanding of quantum leakage from the variational manifold, this method could be used to detect atypical behaviour and absence of maximal scrambling in general models that do not have an obvious large- N limit. One of the ultimate future challenges is to bring together this approach to real-time dynamics with approaches directly targeting the properties of many-body eigenstates. This challenge may be attacked using quantum information techniques, which, for example, allow one to link revivals and eigenstate properties⁹⁶. Related techniques, as well as those used to bound relaxation times from below in prethermal systems, may give crucial insights into the response of quantum many-body scars to perturbations, and their dynamics at long times.

Finally, there is strong experimental and practical interest in quantum many-body scars. Many-body scarred revivals provide a mechanism for maintaining coherence, despite the presence of interactions that normally scramble local quantum information. In particular, scars in Rydberg chains—so far the main experimental realization of the phenomenon—have already been used for the preparation of specific entangled states⁹⁷. This application made use of quantum control based on the variational TDVP approach and its identification of entangled periodic trajectories that simultaneously have small quantum leakage. This suggests that scars may have a wider range of applications, for example, in protected state transfer on quantum networks or in quantum sensing. Such applications require deeper theoretical understanding of the effects that protect the coherence of scars, as well as the development of general experimental techniques for creating them on demand, such as using periodic driving in Rydberg arrays⁹⁸, pumping protocols in dipolar Bose gases⁹⁹ or tilting the Fermi–Hubbard model¹⁰⁰. Looking back at the field of single-particle scars, which have been realized in a multitude of experimental settings, one may also expect many-body quantum scars to be relevant to a much broader family of quantum simulators beyond Rydberg atoms and perhaps even in solid state materials. In all these platforms, quantum many-body scars may serve as a vehicle for controlling and manipulating many-body states, which may prove useful in a range of quantum technology applications. At this stage, the field of weakly broken ergodicity is still in its infancy, and experimental progress will undoubtedly yield more surprises in the near future.

Received: 12 November 2020; Accepted: 18 March 2021;
Published online: 27 May 2021

References

- Bloch, I., Dalibard, J. & Nascimbène, S. Quantum simulations with ultracold quantum gases. *Nat. Phys.* **8**, 267–276 (2012).
- Georgescu, I. M., Ashhab, S. & Nori, F. Quantum simulation. *Rev. Mod. Phys.* **86**, 153–185 (2014).
- Kinoshita, T., Wenger, T. & Weiss, D. S. A quantum Newton's cradle. *Nature* **440**, 900–903 (2006).
- Nandkishore, R. & Huse, D. A. Many-body localization and thermalization in quantum statistical mechanics. *Annu. Rev. Condens. Matter Phys.* **6**, 15–38 (2015).
- Abanin, D. A., Altman, E., Bloch, I. & Serbyn, M. Colloquium: Many-body localization, thermalization, and entanglement. *Rev. Mod. Phys.* **91**, 021001 (2019).
- Deutsch, J. M. Quantum statistical mechanics in a closed system. *Phys. Rev. A* **43**, 2046–2049 (1991).
- Srednicki, M. Chaos and quantum thermalization. *Phys. Rev. E* **50**, 888–901 (1994).
- Bernien, H. et al. Probing many-body dynamics on a 51-atom quantum simulator. *Nature* **551**, 579–584 (2017).
- Turner, C. J., Michailidis, A. A., Abanin, D. A., Serbyn, M. & Papić, Z. Weak ergodicity breaking from quantum many-body scars. *Nat. Phys.* **14**, 745–749 (2018).
- Ho, W. W., Choi, S., Pichler, H. & Lukin, M. D. Periodic orbits, entanglement, and quantum many-body scars in constrained models: matrix product state approach. *Phys. Rev. Lett.* **122**, 040603 (2019).
- Heller, E. J. Bound-state eigenfunctions of classically chaotic hamiltonian systems: scars of periodic orbits. *Phys. Rev. Lett.* **53**, 1515–1518 (1984).
- Labuhn, H. et al. Tunable two-dimensional arrays of single Rydberg atoms for realizing quantum Ising models. *Nature* **534**, 667–670 (2016).
- Lesanovsky, I. & Katsura, H. Interacting Fibonacci anyons in a Rydberg gas. *Phys. Rev. A* **86**, 041601 (2012).
- Sun, B. & Robicheaux, F. Numerical study of two-body correlation in a 1D lattice with perfect blockade. *New J. Phys.* **10**, 045032 (2008).
- Olmos, B., Müller, M. & Lesanovsky, I. Thermalization of a strongly interacting 1D Rydberg lattice gas. *New J. Phys.* **12**, 013024 (2010).
- Turner, C. J., Michailidis, A. A., Abanin, D. A., Serbyn, M. & Papić, Z. Quantum scarred eigenstates in a Rydberg atom chain: entanglement, breakdown of thermalization, and stability to perturbations. *Phys. Rev. B* **98**, 155134 (2018b).
- Michailidis, A. A., Turner, C. J., Papić, Z., Abanin, D. A. & Serbyn, M. Stabilizing two-dimensional quantum scars by deformation and synchronization. *Phys. Rev. Res.* **2**, 022065 (2020).
- Lin, C.-J., Calvera, V. & Hsieh, T. H. Quantum many-body scar states in two-dimensional Rydberg atom arrays. *Phys. Rev. B* **101**, 220304 (2020).
- van Voorden, B., Minář, J. & Schoutens, K. Quantum many-body scars in transverse field Ising ladders and beyond. *Phys. Rev. B* **101**, 220305 (2020).
- Sugiura, S., Kuwahara, T. & Saito, K. Many-body scar state intrinsic to periodically driven system. *Phys. Rev. Res.* **3**, L012010 (2021).
- Mizuta, K., Takasan, K. & Kawakami, N. Exact Floquet quantum many-body scars under Rydberg blockade. *Phys. Rev. Res.* **2**, 033284 (2020).
- Mukherjee, B., Nandy, S., Sen, A., Sen, D. & Sengupta, K. Collapse and revival of quantum many-body scars via Floquet engineering. *Phys. Rev. B* **101**, 245107 (2020).
- Fendley, P., Sengupta, K. & Sachdev, S. Competing density-wave orders in a one-dimensional hard-boson model. *Phys. Rev. B* **69**, 075106 (2004).
- Lesanovsky, I. Liquid ground state, gap, and excited states of a strongly correlated spin chain. *Phys. Rev. Lett.* **108**, 105301 (2012).
- Mondragon-Shem, I., Vavilov, M. G. & Martin, I. The fate of quantum many-body scars in the presence of disorder. Preprint at <https://arxiv.org/abs/2010.10535> (2020).
- Lin, C.-J., Chandran, A. & Motrunich, O. I. Slow thermalization of exact quantum many-body scar states under perturbations. *Phys. Rev. Res.* **2**, 033044 (2020b).
- Lin, C.-J. & Motrunich, O. I. Exact quantum many-body scar states in the Rydberg-blockaded atom chain. *Phys. Rev. Lett.* **122**, 173401 (2019).
- Iadecola, T., Schecter, M. & Xu, S. Quantum many-body scars from magnon condensation. *Phys. Rev. B* **100**, 184312 (2019).
- Barut, A. O. et al. *Dynamical Groups and Spectrum Generating Algebras* Vol. 1 (World Scientific, 1988).
- Yang, C. N. η pairing and off-diagonal long-range order in a Hubbard model. *Phys. Rev. Lett.* **63**, 2144–2147 (1989).
- Shoucheng, Z. Pseudospin symmetry and new collective modes of the Hubbard model. *Phys. Rev. Lett.* **65**, 120–122 (1990).
- Moudgalya, S., Regnault, N. & Bernevig, B. A. Entanglement of exact excited states of Affleck–Kennedy–Lieb–Tasaki models: exact results, many-body scars, and violation of the strong eigenstate thermalization hypothesis. *Phys. Rev. B* **98**, 235156 (2018).
- Arovas, D. P. Two exact excited states for the $s=1$ AKLT chain. *Phys. Lett. A* **137**, 431–433 (1989).
- Moudgalya, S., O'Brien, E., Bernevig, B. A., Fendley, P. & Regnault, N. Large classes of quantum scarred Hamiltonians from matrix product states. *Phys. Rev. B* **102**, 085120 (2020).
- Mark, D. K., Lin, C.-J. & Motrunich, O. I. Unified structure for exact towers of scar states in the Affleck–Kennedy–Lieb–Tasaki and other models. *Phys. Rev. B* **101**, 195131 (2020).
- Vafek, O., Regnault, N. & Bernevig, B. A. Entanglement of exact excited eigenstates of the Hubbard model in arbitrary dimension. *SciPost Phys.* **3**, 043 (2017).
- Moudgalya, S., Regnault, N. & Bernevig, B. A. η -pairing in Hubbard models: from spectrum generating algebras to quantum many-body scars. *Phys. Rev. B* **102**, 085140 (2020).
- Mark, D. K. & Motrunich, O. I. η -pairing states as true scars in an extended Hubbard model. *Phys. Rev. B* **102**, 075132 (2020).
- Schecter, M. & Iadecola, T. Weak ergodicity breaking and quantum many-body scars in spin-1 XY magnets. *Phys. Rev. Lett.* **123**, 147201 (2019).
- Chattopadhyay, S., Pichler, H., Lukin, M. D. & Ho, W. W. Quantum many-body scars from virtual entangled pairs. *Phys. Rev. B* **101**, 174308 (2020).
- Iadecola, T. & Schecter, M. Quantum many-body scar states with emergent kinetic constraints and finite-entanglement revivals. *Phys. Rev. B* **101**, 024306 (2020).
- Shibata, N., Yoshioka, N. & Katsura, H. Onsager's scars in disordered spin chains. *Phys. Rev. Lett.* **124**, 180604 (2020).

43. Lee, K., Melendrez, R., Pal, A. & Changlani, H. J. Exact three-colored quantum scars from geometric frustration. *Phys. Rev. B* **101**, 241111 (2020).
44. Pakrouski, K., Pallegar, P. N., Popov, F. K. & Klebanov, I. R. Many-body scars as a group invariant sector of Hilbert space. *Phys. Rev. Lett.* **125**, 230602 (2020).
45. Ren, J., Liang, C. & Fang, C. Quasi-symmetry groups and many-body scar dynamics. Preprint at <https://arxiv.org/abs/2007.10380> (2020).
46. O’Dea, N., Burnell, F., Chandran, A. & Khemani, V. From tunnels to towers: quantum scars from Lie algebras and q -deformed Lie algebras. *Phys. Rev. Res.* **2**, 043305 (2020).
47. Buča, B., Tindall, J. & Jaksch, D. Non-stationary coherent quantum many-body dynamics through dissipation. *Nat. Commun.* **10**, 1730 (2019).
48. Tindall, J., Buča, B., Coulthard, J. R. & Jaksch, D. Heating-induced long-range η pairing in the Hubbard model. *Phys. Rev. Lett.* **123**, 030603 (2019).
49. Choi, S. et al. Emergent SU(2) dynamics and perfect quantum many-body scars. *Phys. Rev. Lett.* **122**, 220603 (2019).
50. Khemani, V., Laumann, C. R. & Chandran, A. Signatures of integrability in the dynamics of Rydberg-blockaded chains. *Phys. Rev. B* **99**, 161101 (2019).
51. Bull, K., Desaulles, J.-Y. & Papić, Z. Quantum scars as embeddings of weakly broken Lie algebra representations. *Phys. Rev. B* **101**, 165139 (2020).
52. Turner, C. J., Desaulles, J.-Y., Bull, K. & Papić, Z. Correspondence principle for many-body scars in ultracold Rydberg atoms. *Phys. Rev. X* **11**, 021021 (2021).
53. Moudgalya, S., Prem, A., Nandkishore, R., Regnault, N. & Bernevig, B. A. Thermalization and its absence within Krylov subspaces of a constrained Hamiltonian. Preprint at <https://arxiv.org/abs/1910.14048> (2019).
54. Moudgalya, S., Bernevig, B. A. & Regnault, N. Quantum many-body scars in a Landau level on a thin torus. *Phys. Rev. B* **102**, 195150 (2020).
55. Hudomal, A., Vasić, I., Regnault, N. & Papić, Z. Quantum scars of bosons with correlated hopping. *Commun. Phys.* **3**, 99 (2020).
56. Zhao, H., Vovrosh, J., Mintert, F. & Knolle, J. Quantum many-body scars in optical lattices. *Phys. Rev. Lett.* **124**, 160604 (2020).
57. Sala, P., Rakovszky, T., Verresen, R., Knap, M. & Pollmann, F. Ergodicity breaking arising from Hilbert space fragmentation in dipole-conserving Hamiltonians. *Phys. Rev. X* **10**, 011047 (2020).
58. Pai, S. & Pretko, M. Dynamical scar states in driven fracton systems. *Phys. Rev. Lett.* **123**, 136401 (2019).
59. Khemani, V., Hermele, M. & Nandkishore, R. Localization from Hilbert space shattering: from theory to physical realizations. *Phys. Rev. B* **101**, 174204 (2020).
60. Shiraishi, N. & Mori, T. Systematic construction of counterexamples to the eigenstate thermalization hypothesis. *Phys. Rev. Lett.* **119**, 030601 (2017).
61. Surace, F. M., Giudici, G. & Dalmonte, M. Weak-ergodicity-breaking via lattice supersymmetry. *Quantum* **4**, 339 (2020).
62. Kuno, Y., Mizoguchi, T. & Hatsugai, Y. Flat band quantum scar. *Phys. Rev. B* **102**, 241115 (2020).
63. McClarty, P. A., Haque, M., Sen, A. & Richter, J. Disorder-free localization and many-body quantum scars from magnetic frustration. *Phys. Rev. B* **102**, 224303 (2020).
64. Wildeboer, J., Seidel, A., Srivatsa, N. S., Nielsen, A. E. B. & Erten, O. Topological quantum many-body scars in quantum dimer models on the kagome lattice. Preprint at <https://arxiv.org/abs/2009.00022> (2020).
65. Ok, S. et al. Topological many-body scar states in dimensions one, two, and three. *Phys. Rev. Res.* **1**, 033144 (2019).
66. Bull, K., Martin, I. & Papić, Z. Systematic construction of scarred many-body dynamics in 1D lattice models. *Phys. Rev. Lett.* **123**, 030601 (2019).
67. Shiraishi, N. Connection between quantum-many-body scars and the Affleck–Kennedy–Lieb–Tasaki model from the viewpoint of embedded Hamiltonians. *J. Stat. Mech. Theory Exp.* **2019**, 083103 (2019).
68. Dirac, P. A. M. Note on exchange phenomena in the Thomas atom. *Math. Proc. Cambridge Phil. Soc.* **26**, 376–385 (1930).
69. Heller, E. J. Time dependent variational approach to semiclassical dynamics. *J. Chem. Phys.* **64**, 63–73 (1976).
70. Haegeman, J. et al. Time-dependent variational principle for quantum lattices. *Phys. Rev. Lett.* **107**, 070601 (2011).
71. Green, A. G., Hooley, C. A., Keeling, J. & Simon, S. H. Feynman path integrals over entangled states. Preprint at <https://arxiv.org/abs/1607.01778> (2016).
72. Leviatan, E., Pollmann, F., Bardarson, J. H., Huse, D. A. & Altman, E. Quantum thermalization dynamics with matrix-product states. Preprint at <https://arxiv.org/abs/1702.08894> (2017).
73. Michailidis, A. A., Turner, C. J., Papić, Z., Abanin, D. A. & Serbyn, M. Slow quantum thermalization and many-body revivals from mixed phase space. *Phys. Rev. X* **10**, 011055 (2020b).
74. Arnold, V. I. *Mathematical Methods of Classical Mechanics* Vol. 60 (Springer Science Business Media, 2013).
75. Brandino, G. P., Caux, J.-S. & Konik, R. M. Glimmers of a quantum KAM theorem: insights from quantum quenches in one-dimensional Bose gases. *Phys. Rev. X* **5**, 041043 (2015).
76. Nandkishore, R. M. & Sondhi, S. L. Many-body localization with long-range interactions. *Phys. Rev. X* **7**, 041021 (2017).
77. Kormos, M., Collura, M., Takács, G. & Calabrese, P. Real-time confinement following a quantum quench to a non-integrable model. *Nat. Phys.* **13**, 246–249 (2017).
78. Robinson, N. J., James, A. J. A. & Konik, R. M. Signatures of rare states and thermalization in a theory with confinement. *Phys. Rev. B* **99**, 195108 (2019).
79. Yang, Z.-C., Liu, F., Gorshkov, A. V. & Iadecola, T. Hilbert-space fragmentation from strict confinement. *Phys. Rev. Lett.* **124**, 207602a (2020).
80. Castro-Alvaredo, O. A., Lencsés, M., Szécsényi, I. M. & Viti, J. Entanglement oscillations near a quantum critical point. *Phys. Rev. Lett.* **124**, 230601 (2020).
81. Magnifico, G. et al. Real time dynamics and confinement in the \mathbb{Z}_n Schwinger–Weyl lattice model for 1+1 QED. *Quantum* **4**, 281 (2020).
82. Chanda, T., Zakrzewski, J., Lewenstein, M. & Tagliacozzo, L. Confinement and lack of thermalization after quenches in the bosonic Schwinger model. *Phys. Rev. Lett.* **124**, 180602 (2020).
83. Borla, U., Verresen, R., Grusdt, F. & Moroz, S. Confined phases of one-dimensional spinless fermions coupled to Z_2 gauge theory. *Phys. Rev. Lett.* **124**, 120503 (2020).
84. Yang, B. et al. Observation of gauge invariance in a 71-site Bose-Hubbard quantum simulator. *Nature* **587**, 392–396 (2020).
85. Surace, F. M. et al. Lattice gauge theories and string dynamics in Rydberg atom quantum simulators. *Phys. Rev. X* **10**, 021041 (2020b).
86. Celi, A. et al. Emerging two-dimensional gauge theories in Rydberg configurable arrays. *Phys. Rev. X* **10**, 021057 (2020).
87. Pancotti, N., Giudice, G., Cirac, J. I., Garrahan, J. P. & Bañuls, M. C. Quantum East model: localization, nonthermal eigenstates, and slow dynamics. *Phys. Rev. X* **10**, 021051 (2020).
88. Roy, S. & Lazarides, A. Strong ergodicity breaking due to local constraints in a quantum system. *Phys. Rev. Res.* **2**, 023159 (2020).
89. Lan, Z., van Horssen, M., Powell, S. & Garrahan, J. P. Quantum slow relaxation and metastability due to dynamical constraints. *Phys. Rev. Lett.* **121**, 040603 (2018).
90. Feldmeier, J., Pollmann, F. & Knap, M. Emergent glassy dynamics in a quantum dimer model. *Phys. Rev. Lett.* **123**, 040601 (2019).
91. Hart, O., De Tomasi, G. & Castelnovo, C. From compact localized states to many-body scars in the random quantum comb. *Phys. Rev. Res.* **2**, 043267 (2020).
92. Hallam, A., Morley, J. G. & Green, A. G. The Lyapunov spectra of quantum thermalisation. *Nat. Commun.* **10**, 2708 (2019).
93. Sachdev, S. & Ye, J. Gapless spin-fluid ground state in a random quantum Heisenberg magnet. *Phys. Rev. Lett.* **70**, 3339–3342 (1993).
94. Kitaev, A. A simple model of quantum holography. Talk at KITP. *Univ. California Santa Barbara* <https://online.kitp.ucsb.edu/online/entangled15/kitaev/> (2015).
95. Maldacena, J., Shenker, S. H. & Stanford, D. A bound on chaos. *J. High Energy Phys.* **2016**, 106 (2016).
96. Alhambra, A. M., Anshu, A. & Wilming, H. Revivals imply quantum many-body scars. *Phys. Rev. B* **101**, 205107 (2020).
97. Omran, A. et al. Generation and manipulation of Schrödinger cat states in Rydberg atom arrays. *Science* **365**, 570–574 (2019).
98. Bluvstein, D. et al. Controlling many-body dynamics with driven quantum scars in Rydberg atom arrays. *Science* <https://doi.org/10.1126/science.abg2530> (2021).
99. Kao, W., Li, K.-Y., Lin, K.-Y., Gopalakrishnan, S. & Lev, B. L. Creating quantum many-body scars through topological pumping of a 1D dipolar gas. Preprint at <https://arxiv.org/abs/2002.10475> (2020).
100. Scherg, S. et al. Observing non-ergodicity due to kinetic constraints in tilted Fermi-Hubbard chains. Preprint at <http://arxiv.org/abs/2010.12965> (2020).
101. Heller, E. J. in *Chaos and Quantum Physics* Vol. 52 (eds Giannoni, M. J. et al.) 547–661 (North-Holland, 1991).
102. Berry, M. V. in *Chaotic Behaviour of Deterministic Systems* Vol. 36 (eds Chenciner, A. et al.) 171–271 (North-Holland, 1983).
103. Sridhar, S. Experimental observation of scarred eigenfunctions of chaotic microwave cavities. *Phys. Rev. Lett.* **67**, 785–788 (1991).
104. Wilkinson, P. B. et al. Observation of “scarred” wavefunctions in a quantum well with chaotic electron dynamics. *Nature* **380**, 608–610 (1996).
105. Wintgen, D. & Hönig, A. Irregular wave functions of a hydrogen atom in a uniform magnetic field. *Phys. Rev. Lett.* **63**, 1467–1470 (1989).

Acknowledgements

We thank our collaborators K. Bull, S. Choi, J.-Y. Desaulles, W. W. Ho, A. Hudomal, M. Lukin, I. Martin, H. Pichler, N. Regnault, I. Vasić and in particular A. Michailidis and C. Turner, without whom this work would not have been possible. We also benefited from discussions with E. Altman, B. A. Bernevig, A. Chandran, P. Fendley, V. Khemani

and L. Motrunich. M.S. was supported by the European Research Council (ERC) under the European Union's Horizon 2020 research and innovation programme (grant agreement no. 850899). D.A.A. was supported by the Swiss National Science Foundation and by the ERC under the European Union's Horizon 2020 research and innovation programme (grant agreement no. 864597). Z.P. acknowledges support by the Leverhulme Trust Research Leadership Award RL-2019-015.

Competing interests

The authors declare no competing interests.

Additional information

Correspondence should be addressed to Z.P.

Peer review information *Nature Physics* thanks the anonymous reviewers for their contribution to the peer review of this work.

Reprints and permissions information is available at www.nature.com/reprints.

Publisher's note Springer Nature remains neutral with regard to jurisdictional claims in published maps and institutional affiliations.

© Springer Nature Limited 2021